

Resonance Stabilized Bisdiselenazolyis as Neutral Radical Conductors

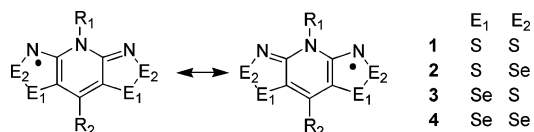
Jaclyn L. Brusso, Kristina Cvrkalj, Alicea A. Leitch, Richard T. Oakley,* Robert W. Reed, and Craig M. Robertson

Department of Chemistry, University of Waterloo, Waterloo, Ontario N2L 3G1, Canada

Received September 15, 2006; E-mail: oakley@uwaterloo.ca

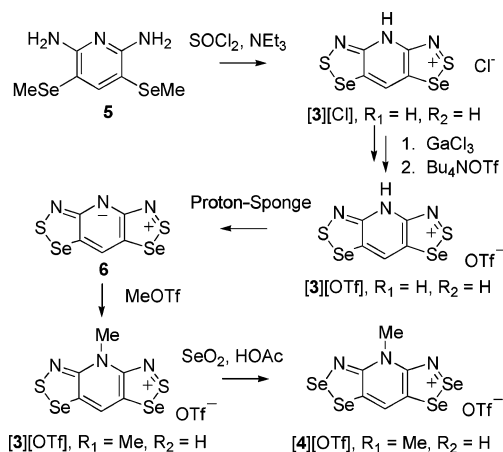
Heterocyclic thiazyl radicals hold considerable potential in the design of both conductive and magnetic materials.¹ In the pursuit of improved conductivity we developed a series of radicals based on the bis-1,2,3-dithiazolyl framework **1** (Chart 1, $E_1 = E_2 = S$).^{2–4} These resonance stabilized systems enjoy lower molecular disproportionation energies ΔH_{disp} and cell potentials E_{cell} than their monofunctional counterparts and, as a result, a reduced solid-state on-site Coulomb repulsion U . However, the steric bulk of the substituents R_1 and R_2 forces the radicals to crystallize in slipped rather than superimposed π -stack arrays. The resultant loss in intermolecular overlap between neighboring radicals reduces the bandwidth W of the associated half-filled energy band, and a Mott insulating ground state prevails. One approach to improving W is to incorporate selenium in place of sulfur. Sequential replacement of sulfur by selenium affords, in principle, the three selenium based radicals **2–4**. We recently described methods for the partial introduction of selenium, as in **2**,⁵ but to date methods to access the isomeric mixed S/Se materials **3** and the all-selenium radicals **4** have been elusive. Herein we report the preparation and solid-state characterization of the first examples of **3** and **4** (with $R_1 = \text{Me}$, $R_2 = \text{H}$).

Chart 1



The critical intermediate in the synthetic sequence (Scheme 1) to both **3** and **4** is diamino-bis(methylseleno)-pyridine **5**. This material is readily generated by reduction ($\text{NaBH}_4/\text{MeOH}$) and methylation (MeI) of the diaminopyridine-bis(selenocyanate), which itself is prepared in a manner analogous to that used for the corresponding bis(thiocyanate).^{3b} Subsequent cleavage of the Se–C(methyl) bonds of **5** and ring closure to the desired heterocyclic framework can be effected with an excess of thionyl chloride⁶ in the presence of triethylamine, using MeCN as solvent. The resulting black, insoluble chloride salt **[3][Cl]** ($R_1 = R_2 = \text{H}$) is purified by conversion to a tetrachlorogallate and metathesis of the latter to a trifluoromethanesulfonate or triflate (OTf^-) salt. Deprotonation of green solutions of **[3][OTf]** ($R_1 = R_2 = \text{H}$) in MeCN with Proton-Sponge affords the zwitterion **6** as a green insoluble powder. Treatment of **6** with methyl triflate in DCE yields a sparkling red precipitate of the *N*-methyl salt **[3][OTf]** ($R_1 = \text{Me}$, $R_2 = \text{H}$), which crystallizes from hot glacial acetic acid as red needles, $\lambda_{\text{max}}(\text{MeCN}) = 700 \text{ nm}$ ($\log \epsilon = 4.6$). Finally, conversion of **[3][OTf]** ($R_1 = \text{Me}$, $R_2 = \text{H}$) to **[4][OTf]** ($R_1 = \text{Me}$, $R_2 = \text{H}$) can be achieved by boiling the former in glacial acetic acid in the presence of SeO_2 .^{5c} Recrystallization of **[4][OTf]** ($R_1 = \text{Me}$, $R_2 = \text{H}$) from MeCN affords deep red flakes, $\lambda_{\text{max}}(\text{MeCN}) = 736 \text{ nm}$ ($\log \epsilon = 4.7$).

Scheme 1



Chemical reduction of the salts **[3][OTf]** and **[4][OTf]** to the respective radicals **3** and **4** ($R_1 = \text{Me}$, $R_2 = \text{H}$) was achieved with octamethylferrocene in MeCN. Single-crystal X-ray analysis⁷ of the bronze needles of **3** established that it is essentially isostructural with **1** ($R_1 = \text{Me}$, $R_2 = \text{H}$),³ both compounds belonging to the orthorhombic space group $P2_12_12_1$ and differing only in the sense of their chirality. In the case of **4**, however, the radical precipitates as brown microcrystals unsuitable for single crystal work. X-ray powder diffraction measurements on this material, followed by Rietveld analysis starting from the coordinates and the space group of **3**,⁷ nonetheless allowed us to confirm that this compound is also isostructural with **1** and **3**. A drawing of the unit cell of **4** is shown in Figure 1. Table 1 provides the unit cell parameters of the three isostructural radicals and also provides a summary of the pertinent intermolecular $E \cdots E'$ contacts ($E = \text{S}, \text{Se}$).

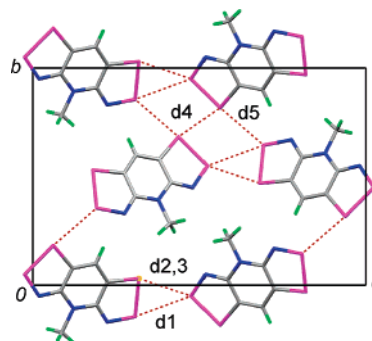


Figure 1. Unit cell of **4** ($R_1 = \text{Me}$, $R_2 = \text{H}$), showing intermolecular $\text{Se} \cdots \text{Se}'$ contacts.

In contrast to **2** ($R_1 = \text{Me}$, $R_2 = \text{H}$), which associates in the solid state as laterally Se–Se σ -bonded dimers,^{5b} all three radicals **1**, **3**, and **4** ($R_1 = \text{Me}$, $R_2 = \text{H}$) crystallize in an undimerized fashion, the discrete radicals packing in slipped π -stack arrays along the

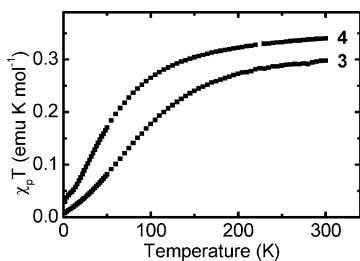
Table 1. Crystal Data and Intermolecular Contacts d1–d5

radical ^a	1 ^b	3	4
<i>a</i> , Å	3.9626(10)	4.11070(4)	4.199(5)
<i>b</i> , Å	11.962(3)	11.79530(10)	12.181(13)
<i>c</i> , Å	18.262(5)	18.6524(2)	18.64(2)
d1, Å	3.371(1)	3.494(1)	3.479(3)
d2, Å	3.666(1)	3.604(1)	3.692(3)
d3, Å	3.745(1)	3.790(1)	3.834(3)
d4, Å	3.437(1)	3.473(1)	3.561(2)
d5, Å	3.394(1)	3.314(1)	3.335(2)

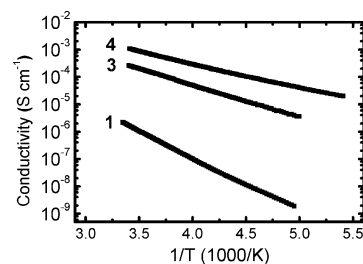
^a R₁ = Me, R₂ = H. ^b Reference 3a.

x-direction. These arrays are linked into ribbons running parallel to the *z*-direction by a series of close E···E' contacts d1–d3. In addition, there are two E···E' interactions d4 and d5 that bridge neighboring ribbons along the *y*-direction. Collectively, this network of intermolecular interactions generates a closely knit and relatively three-dimensional electronic structure.

The very low solubility of **3** and **4** (R₁ = Me, R₂ = H) in organic solvents precludes their characterization by solution-based EPR methods. Solid-state magnetic measurements as a function of temperature have been performed on both compounds. These experiments confirm that the radicals are not spin paired in the solid state. Plots of $\chi_p T$ versus *T*, where χ_p is the magnetic susceptibility corrected for diamagnetic contributions, are shown in Figure 2. In both cases $\chi_p T$ approaches 0.375 near room temperature, as expected for undimerized *S* = 1/2 systems, but at lower temperatures its value drops steadily, indicative of strong antiferromagnetic intermolecular coupling. Curie-Weiss fits to the high-temperature data (above 160 K for **3** and above 100 K for **4**) afforded Curie constants *C* = 0.377 and 0.392 emu K mol⁻¹, and θ -values of -78.3 and -44.3 K for **3** and **4**, respectively. By contrast, the all-sulfur radical **1** (R₁ = Me, R₂ = H) exhibited essentially paramagnetic behavior, with weak ferromagnetic coupling at very low temperatures.³

**Figure 2.** Plots of $\chi_p T$ vs *T* for **3** and **4** (R₁ = Me, R₂ = H).

Previous four-probe single-crystal conductivity (σ) measurements on **1** (R₁ = Me, R₂ = H) as a function of temperature indicated Mott insulator behavior, with a room-temperature conductivity $\sigma(295\text{ K}) = 2 \times 10^{-6}\text{ S cm}^{-1}$ and thermal activation energy $E_{\text{act}} = 0.41\text{ eV}$.³ The results of four-probe pressed pellet measurements on **3** and **4** (R₁ = Me, R₂ = H) are illustrated in Figure 3. Sequential incorporation of selenium leads to progressive improvement in the conductivity, with $\sigma(295\text{ K}) = 3 \times 10^{-4}$ and $1 \times 10^{-3}\text{ S cm}^{-1}$ for **3** and **4**, respectively. At the same time the value of E_{act} is reduced to 0.24 eV in **3** and 0.17 eV in **4**.

**Figure 3.** Conductivity of **1**, **3**, and **4** (R₁ = Me, R₂ = H) as a function of inverse temperature. Data for **1** are from ref 3b.

In summary, we have developed a general synthetic route to the all-selenium based resonance stabilized radicals **4**. Structural analyses on **3** and **4** (R₁ = Me, R₂ = H) confirm that lattice and π -delocalization energies are sufficient to prevent solid-state dimerization of the radicals. Incorporation of selenium leads to a dramatic increase in conductivity and reduction in thermal activation energy relative to sulfur based radicals. Modification of the R₁/R₂ groups and/or the application of physical pressure, as found for derivatives of **2**,^{5c} may well lead to an even better performance, and perhaps a metallic state.

Acknowledgment. We thank the NSERC (Canada) for financial support. We also thank the Canada Council for the Arts for a Killam Fellowship to R.T.O. and the NSERC and the Ontario Provincial Government for postgraduate scholarships to A.A.L. and J.L.B.

Supporting Information Available: Experimental procedures, π -stacking diagram of **4**, and crystallographic data in CIF format for **3** and **4**. This material is available free of charge via the Internet at <http://pubs.acs.org>.

References

- (1) (a) Rawson, J. M.; Alberola, A.; Whalley, A. *J. Mater. Chem.* **2006**, *16*, 2560. (b) Awaga, K.; Tanaka, T.; Shirai, T.; Fujimori, M.; Suzuki, Y.; Yoshikawa, H.; Fujita, W. *Bull. Chem. Soc. Jpn.* **2006**, *79*, 25.
- (2) Beer, L.; Brusso, J. L.; Cordes, A. W.; Haddon, R. C.; Itkis, M. E.; Kirschbaum, K.; MacGregor, D. S.; Oakley, R. T.; Pinkerton, A. A.; Reed, R. W. *J. Am. Chem. Soc.* **2002**, *124*, 9498.
- (3) (a) Beer, L.; Brusso, J. L.; Cordes, A. W.; Haddon, R. C.; Godde, E.; Itkis, M. E.; Oakley, R. T.; Reed, R. W. *Chem. Commun.* **2002**, 2562. (b) Beer, L.; Britten, J. F.; Brusso, J. L.; Cordes, A. W.; Haddon, R. C.; Itkis, M. E.; MacGregor, D. S.; Oakley, R. T.; Reed, R. W.; Robertson, C. M. *J. Am. Chem. Soc.* **2003**, *125*, 14394.
- (4) Beer, L.; Britten, J. F.; Clements, O. P.; Haddon, R. C.; Itkis, M. E.; Matkovich, K. M.; Oakley, R. T.; Reed, R. W. *Chem. Mater.* **2004**, *16*, 1564.
- (5) (a) Beer, L.; Brusso, J. L.; Haddon, R. C.; Itkis, M. E.; Leitch, A. A.; Oakley, R. T.; Reed, R. W.; Richardson, J. F. *Chem. Commun.* **2005**, 1543. (b) Beer, L.; Brusso, J. L.; Haddon, R. C.; Itkis, M. E.; Kleinke, H.; Leitch, A. A.; Oakley, R. T.; Reed, R. W.; Richardson, J. F.; Secco, R. A.; Yu, X. *J. Am. Chem. Soc.* **2005**, *127*, 1815. (c) Beer, L.; Brusso, J. L.; Haddon, R. C.; Itkis, M. E.; Oakley, R. T.; Reed, R. W.; Richardson, J. F.; Secco, R. A.; Yu, X. *Chem. Commun.* **2005**, 5745.
- (6) Reich, H. J.; Wollowitz, S. *J. Am. Chem. Soc.* **1982**, *104*, 7051.
- (7) Crystal data for **3** at 298(2) K: C₆H₄N₃S₂Se₂, MW = 340.16, orthorhombic; space group *P2₁2₁2₁*, with *a* = 4.11070(4), *b* = 11.79530(10), *c* = 18.6524(2) Å, *V* = 904.398(12) Å³, *Z* = 4, *D*_{calcd} = 2.498 g cm⁻³, μ = 14.154 mm⁻¹; 123 parameters were refined using 1588 unique reflections to give *R* = 0.0213 and *R*_w = 0.0579. Crystal data for **4** at 298(2) K: C₆H₄N₃Se₄, MW = 433.96; orthorhombic, space group *P2₁2₁2₁*, with *a* = 4.199(5), *b* = 12.181(13), *c* = 18.64(2) Å, *V* = 953.1(18) Å³, *Z* = 4, *D*_{calcd} = 3.024 g cm⁻³. Powder X-ray data analysed by Rietveld methods based on the coordinates and space group of **3**, allowing for full anisotropic refinement of the selenium atoms and isotropic refinement of all other non-hydrogen atoms gave *R*_p = 0.0629 and *wR*_p = 0.0782.

JA0666856